Neurogenesis Dynamics-inspired Spiking Neural Network Training Acceleration

Shaoyi Huang [1], Haowen Fang, Kaleel Mahmood [1], Bowen Lei [2], Nuo Xu [3], Bin Lei [1], Yue Sun [3], Dongkuan Xu [4], Wujie Wen [3], Caiwen Ding [1]
[1]University of Connecticut, [2]Texas A&M University, [3]Lehigh University, [4]North Carolina State University
{shaoyi.huang, kaleel.mahmood, bin.lei, caiwen.ding}@uconn.edu,
bowenlei@stat.tamu.edu, {nux219, yus516, wuw219}@lehigh.edu, dxu27@ncsu.edu

***Abstract*—Biologically inspired Spiking Neural Networks (SNNs) have attracted significant attention for their ability to provide extremely energy-efficient machine intelligence through event-driven operation and sparse activities. As artificial intelligence (AI) becomes ever more democratized, there is an increasing need to execute SNN models on edge devices. Existing works adopt weight pruning to reduce SNN model size and accelerate inference. However, these methods mainly focus on how to obtain a sparse model for efficient inference, rather than training efficiency. To overcome these drawbacks, in this paper, we propose a Neurogenesis Dynamics-inspired Spiking Neural Network training acceleration framework, NDSNN. Our framework is computational efficient and trains a model from scratch with dynamic sparsity without sacrificing model fidelity. Specifically, we design a new drop-and-grow strategy with decreasing number of non-zero weights, to maintain extreme high sparsity and high accuracy. We evaluate NDSNN using VGG-16 and ResNet-19 on CIFAR-10, CIFAR-100 and TinyImageNet. Experimental results show that NDSNN achieves up to 20.52% improvement in accuracy on Tiny-ImageNet using ResNet-19 (with a sparsity of 99%) as compared to other SOTA methods (e.g., Lottery Ticket Hypothesis (LTH), SET-SNN, RigL-SNN). In addition, the training cost of NDSNN is only 40.89% of the LTH training cost on ResNet-19 and 31.35% of the LTH training cost on VGG-16 on CIFAR-10.**

***Index Terms*—spiking neural network, neural network pruning, sparse training, neuromorphic computing**

I. Introduction

Biologically inspired Spiking Neural Networks (SNNs) have attracted significant attention for their ability to provide extremely energy-efficient machine intelligence. SNNs achieve this performance through event-driven operation (e.g., computation is only performed on demand) and the sparse activities of spikes. As artificial intelligence (AI) becomes ever more democratized, there is an increasing need to execute machine learning models on edge devices with limited memory and restricted computational resources [1, 2]. However, modern SNNs typically consist of at least millions to hundreds of millions of parameters (i.e., weights), which requires large memory storage and computations [3, 4, 5]. Therefore, it is desirable to investigate efficient implementation techniques for SNNs.

Recently, the use of sparsity to compress SNN model size and accelerate inference has attracted a surge of attention [6, 7], including the train-prune-retrain method (e.g, alternating direction method of multipliers (ADMM) pruning [6, 8, 9, 10]), iterative pruning (e.g., lottery ticket hypothesis (LTH) [7, 11])). The aforementioned methods are shown in Fig. 1 and mainly focus on how to obtain a sparse model for efficient inference. However, the training process to obtain a sparse model is not efficient. To illustrate consider the case VGG-16 on CIFAR-10,

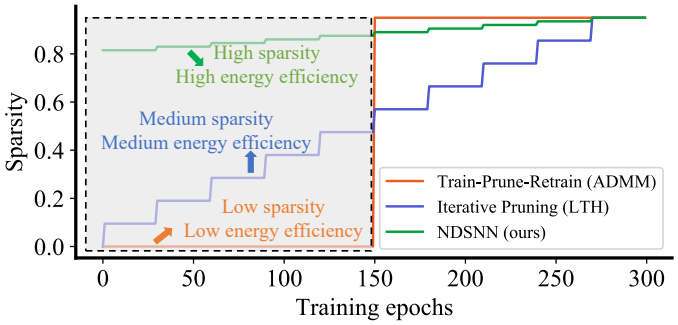

Fig. 1: Sparsity change of different sparsification methods on VGG-16 / ResNet-19 CIFAR-10.

for train-prune-retrain [6, 12] (orange line), the first 150 training epoches are dense (zero sparsity); For iterative pruning [7], the sparsity gradually increases in the first 150 training epoches. As shown in the highlighted grey area, both methods have low sparsity hence low training efficiency.

In the field of neuroscience, the total number of neurons declines with age during the process of neuron's degeneration (i.e., old neuron's death) and redifferentiation (i.e., new neuron's birth), in human hippocampus, referred as Neurogenesis Dynamics [13, 14]. In this paper, inspired by the Neurogenesis Dynamics, we propose an efficient Spiking Neural Network training acceleration framework, NDSNN. We analogize the neuron's death-and-birth renewal scheme to the drop-and-grow schedule in SNN sparse training. We dynamically reduce the number of neuron connections in SNN sparse training, to reduce training memory footprint and improve training efficiency [15]. The number of zeros decreases in the dynamically changing process of weight mask tensor (i.e., a binary tensor which has the same size as weight, 0s / 1s denotes zeros / non-zeros in corresponding weight tensor). The sparsity during NDSNN training is illustrated in Fig. 1 as the green curve. We could train from a highly sparsified model (e.g., initial sparsity is 80%) and achieve the final sparsity (e.g., 95%).

Overall our paper makes the following contributions:

- Inspired by neurogenesis dynamics, we propose an energy efficient spiking neural network training workflow.

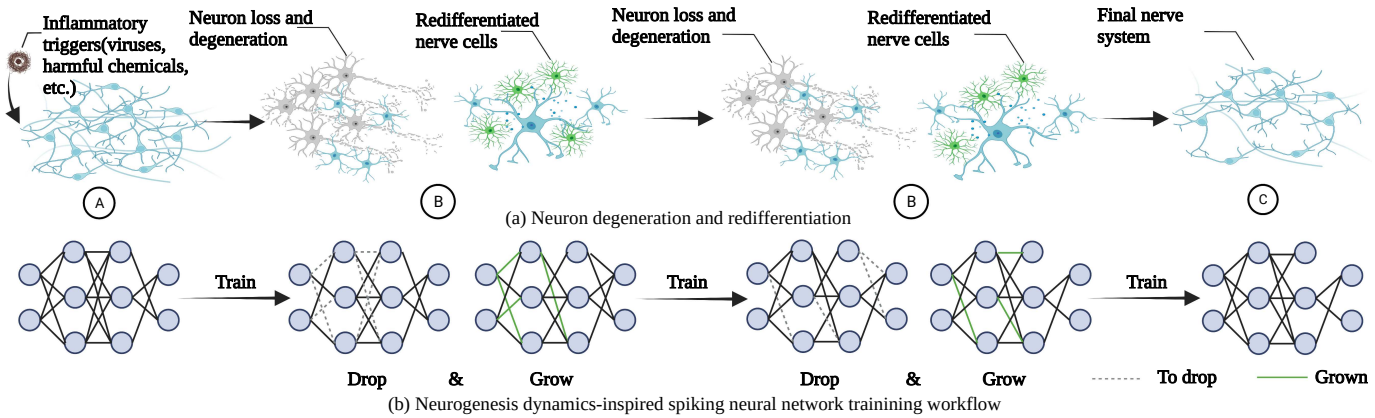

(a) Neuron degeneration and redifferentiation

(b) Neurogenesis dynamics-inspired spiking neural network trainining workflow

Fig. 2: (a) shows the neurogenesis dynamics of nerve cells in the nervous system. A indicates inflammatory factors accumulating in nerve system. B indicates neuron degeneration and redifferentiation process. C is the final nerve system. (b) shows drop and grow process of the neural network. The total number of nonzero weights decreases with the increasing of drop-and-grow times.

- To reach high sparsity and high energy efficiency with dense model like accuracy, we design a new drop-and-grow strategy with decreasing number of non-zero weights in the process of dynamically updating sparse mask.
- We evaluate the training efficiency of NDSNN via normalizing spike rate. Results show that the cost of NDSNN on ResNet-19 and VGG-16 is 40.89% and 31.35% of state-of-the-art (SOTA), respectively.
- We demonstrate extremely high sparsity (i.e., 99%) model performance in SNN based vision tasks with acceptable accuracy degradation.

We evaluate NDSNN using VGG-16 and ResNet on CIFAR-10, CIFAR-100 and TinyImageNet. Experimental results show that NDSNN achieves even high accuracy than dense model for ResNet-19 on CIFAR-10. On Tiny-ImageNet, NDSNN achieves up to 20.52% increase in accuracy compared to the SOTA at a sparsity of 99%. The training cost of NDSNN VGG-16 is 10.5% of training a dense model.

II. Related Work and Background

A. Related Work on Sparsity Exploration in SNN

Several network compression schemes for SNNs have been proposed. In [6] the alternating direction method of multipliers (ADMMs) pruning is employed to compress the SNNs on various datasets. However, this technique has significant accuracy loss, especially when the model has high sparsity. Although IMP could find highly sparse neural network with high accuracy, it is time consuming (e.g. it takes 2720 epochs to achieve 89.91% sparsity on both CIFAR-10 and CIFAT-100) [7]. In [16] they propose a Spike Timing Dependent Plasticity (STDP) based pruning method. Connections between pre-synaptic and post-synaptic neurons with low spike correlation are pruned. The correlation is tracked by STDP algorithm. The performance of this method is limited as the original model only achieves 93.2% accuracy on MNIST, and accuracy drops to 91.5% after 92% weights are pruned. In [17] they propose a technique to prune connections during training. Weights will be pruned if they are less than a certain threshold or decrease significantly in a number of training iterations. However, the method's evaluation is limited, as it is only tested on a single dataset Caltech-101.

B. Spiking Neural Network

A key difference of SNN from DNN is that spiking neuron is a stateful system that can be modeled by different equations. The commonly used Leaky Integrate and Fire (LIF) spiking neuron is defined as follows.

$$v[t] = \alpha v[t-1] + \sum_i w_i s_i[t] - \vartheta o[t-1] \tag{1a}$$

$$o[t] = u(v[t] - \vartheta) \tag{1b}$$

$$u(x) = 0, x < 0 \text{ otherwise } 1 \tag{1c}$$

where t indicates time. Eq. (1a) depicts the dynamics of the neuron's membrane potential $v[t]$. $\alpha \in (0,1]$ determines $v[t]$ the decay speed. $s_i[t] \in \{0,1\}$ is a sequence which consists of only 0 and 1 to represent the $i-th$ input spike train and w_i is the corresponding weight. $o[t] \in \{0,1\}$ is the neuron's output spike train, $u(x)$ is the Heaviside step function.

Note that Eq. (1a) is recursive in the temporal domain, so it is possible to use Backpropagation Through Time (BPTT) to train SNNs. However, an issue arises with Eq. (1c), whose derivative is the Dirac Delta function $\Delta(x)$. To overcome this, surrogate gradient method can be used [18] so that the derivative of $u(x)$ is approximated by the derivative of a smooth function. In the forward pass, the SNN still outputs spikes, while in backward pass, $\Delta(x)$ is replaced by a surrogate function so the Heaviside step function has an approximate derivative.

The BPTT for SNNs using a surrogate gradient is derived as follows. Let L be the loss, $\delta_l[t]=\frac{\partial L}{\partial o_l[t]}$ be the error signal at layer l time step t, $\epsilon_l[t]=\frac{\partial L}{\partial v_l[t]}$. $\delta_l[t]$ is propagated recursively as following rules, and gradient of l^{th} layer weight w_l is calculated using Eq. (3).

$$\delta_l[t] = \epsilon_{l+1}[t] w_{l+1} \tag{2a}$$

$$\epsilon_l[t] = \delta_l[t]\phi_l[t] + \alpha\epsilon_l[t] \tag{2b}$$

$$\frac{\partial L}{\partial w_l} = \sum_{t=0}^{T-1} \epsilon_l[t] \cdot [s_l[t]]^\intercal \tag{2c}$$

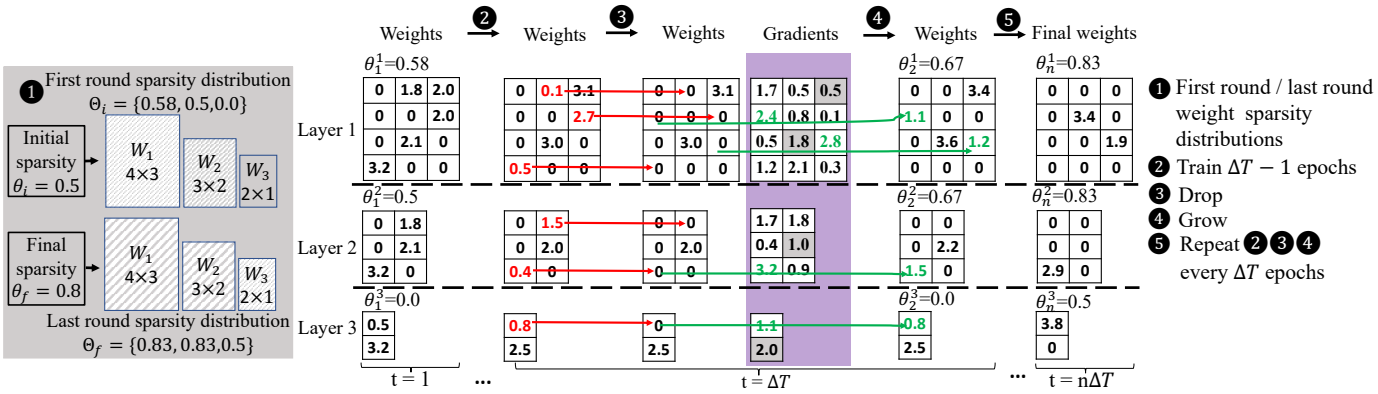

Fig. 3: A toy example of NDSNN training process. Red arrows denote dropping weights and green arrows denote growing weights.

where $\phi_l[t]=\frac{\partial o_l[t]}{\partial v_l[t]}=\frac{\partial u(v_l[t]-\vartheta)}{\partial v_l[t]}$. Note that $u(x)$ does not have a well-defined derivative, so we use the gradient surrogate function proposed in [19] to approximate it, such that:

$$\frac{\partial u(x)}{\partial x} \approx \frac{1}{1+\pi^2 x^2} \tag{3}$$

III. Neurogenesis Dynamics-inspired Sparse Training on SNN

We illustrate the overall workflow of the biological and corresponding computational methods in Fig. 2.

A. Analogizing Neurogenesis Dynamics in Sparse Training

In human hippocampus, the total number of neurons declines with age during the process of neuron's degeneration (i.e., old neuron's death) and redifferentiation (i.e., neuron's birth) [14]. We analogize the neuron's death-and-birth renewal scheme to the drop-and-grow schedule in sparse training [20, 21, 22, 23]. Here *drop* means the insignificant connections are deactivated (weights with least absolute magnitude are set as zeros). In our formulation *grow* refers to creating new connections (weights with high importance are updated to nonzeros). For the dynamics of neurogenesis in the human hippocampus, the neurons declines with age [14]. Similarily in our framework, we reduce the number of connections or reduce the number of activated weights in the sparse training process in consideration of the memory limitation of neuromorphic chips [15].

B. Problem Definiton

We aim to achieve high sparsity (low memory overhead) during training and high energy efficiency (through SNN implementation) without noticeable accuracy loss. The problem is formally defined as: consider a L-layer SNN with dense weights $W = [W_1, W_2, ..., W_L]$, a dataset $\mathcal{X}$, and a target sparsity θ_f, our goal is to develop an training workflow such that the training process requires less memory overhead and less computation, and the trained model achieves high accuracy.

C. Neurogenesis Dynamics-inspired Spiking Neural Network (NDSNN) Training Acceleration Framework

Fig. 2 shows the overview of neurogenesis dynamics-inspired spiking neural network (NDSNN) workflow. Fig. 2(a) demonstrates the neuron cell loss or degeneration (the grey neuron cells) and redifferentiation process (the green neuron cells). In Fig. 2(b) we illustrate the training process of NDSNN, where we drop the weights (i.e., setting the smallest positive weights and the largest negative weights as zeros) in grey color and grow the weights (i.e., update the zeros weights to nonzeros) in green color, every ΔT iterations. The number of weights we dropped is larger than the grown ones each drop-and-grow schedule. Thus, the number of nonzero weights decreases with the increasing of drop-and-grow times.

The goal of the proposed training method is to reduce memory footprint and computations during the whole training process. To achieve it, our proposed method uses less weights and gradients than SOTA methods via dynamically updating the sparse mask and training from scratch. Specifically, we denote θ_i and θ_f as the initial and target sparsity, respectively. t_0 is the starting step of training, ΔT is the pruning frequency. The full training workflow is be formed in the following steps.

❶ **First round / last round weight sparsity distributions across different layers.** Let $\Theta_i = \theta_i^1, \theta_i^2, ..., \theta_i^L$ denote the initial sparsity distribution (i.e., sparsity of different layers at the beginning of training) of SNN model and $\Theta_f = \theta_f^1, \theta_f^2, ..., \theta_f^L$ denote the final sparsity distribution (i.e., sparsity of different layers at the end of training) of the model. Here, we use ERK [24] to distributing the non-zero weights across the layers while maintaining the overall sparsity. We denote n^l as the number of neurons at l-th layer and w^l, h^l as the width and height of the l-th convolutional kernel,then the number of parameters of the sparse convolutional layers are scaled proportional to $1 - \frac{n^{l-1}+n^l+w^l+h^l}{n^{l-1}*n^l*w^l*h^l}$. In our case, the overall sparsity at the beginning of training θ_i is less than the one at the end of training θ_f. Following the same scaling proportion distribution, the sparsity of each separate convolutional layer at the beginning of training is smaller than it's sparsity at the end of training (i.e., for l-th layer, we have $\theta_i^l \leq \theta_f^l$). The sparsity of l-th layer at t-th iteration is formulated as:

$$\theta_t^l = \theta_f^l + (\theta_i^l - \theta_f^l)(1 - \frac{t - t_0}{n\Delta t})^3, \\ t \in \{t_0, t_0 + \Delta T, ..., t_0 + n\Delta T\}, l \in \{1, 2, ..., L\}. \tag{4}$$

❷ **Training.** We define non-active weights as weights has value of zeros and active weights as weights has value of non-zeros. For each iteration, we only update the active weights.

In backward path, gradients are calculated using BPTT with surrogate gradient method, and forward pass is carried out like standard neural network training.

❸ **Dropping (neuron death).** During training, the sparse masks are updated every ΔT iteration, i.e., for l-th layer, we drop D_d^l weights that are closest to zero (i.e., the smallest positive weights and the largest negative weights). we denote d_0 as the initial death ratio (i.e., the ratio of weights to prune from non-zeros) and d_t as the death ratio at step t. We use the cosine annealing learning rate scheduler [25] for death ratio updating. Then, we have

$$\begin{aligned} d_t =& d_{min} + 0.5(d_0 - d_{min})(1 + cos(\frac{\pi t}{n\Delta t})), \\ & t \in \{t_0, t_0 + \Delta T, ..., t_0 + n\Delta T\}, \end{aligned} \tag{5}$$

where d_{min} is the minimum death rate during the training. At q^{th} round, the number of 1s in sparse mask of l-th layer ${N_{pre}}_q^l$ before dropping is

$${N_{pre}}_q^l = N^l(1 - \theta_{q-1}^l), 1 \leq q \leq n, l \in \{1, 2, ..., L\} \tag{6}$$

where N^l is the number of all weight elements in l-th layer and θ_{q-1}^l is the training sparsity of l-th layer at $(q-1)$-th round. We denote the number of dropped weights of l-th layer at q-th round as D_q^l, then, we have

$$D_q^l = d_t \times {N_{pre}}_q^l, 1 \leq q \leq n, l \in \{1, 2, ..., L\}. \tag{7}$$

❹ **Growing (neuron birth).** After dropping weights, the number of 1s in l-th layer sparse mask ${N_{post}}_q^l$ is

$${N_{post}}_q^l = {N_{pre}}_q^l - D_q^l, 1 \leq q \leq n, l \in \{1, 2, ..., L\}. \tag{8}$$

Combining Equation 4 and 8, we obtain the number of weights to be grown, which is denoted as G_q^l, we have

$$G_q^l = N^l - {N_{post}}_q^l - \theta_t^l \times N^l, 1 \leq q \leq n, l \in \{1, 2, ..., L\}. \tag{9}$$

The toy example of the training process is shown in Fig. 3.

Algorithm 1: NDSNN training flow.

Input: a L-layer SNN model g with dense weight $\mathbf{W} = \mathbf{W}_1, \mathbf{W}_2, ..., \mathbf{W}_L$, input data $\mathcal{X}$, update frequency ΔT, initial sparsity θ_i, final sparsity θ_f, learning rate α, total number of training iterations T_{end}.
Set $\mathbf{M}_1, \mathbf{M}_2, ..., \mathbf{M}_L$ as the sparse masks.
Output: a L-layer sparse network with sparsity distribution P_f.
Calculate $\Theta_i = \theta_i^1, \theta_i^2, ..., \theta_i^L$ and $\Theta_f = \theta_f^1, \theta_f^2, ..., \theta_f^L$ using initial sparsity θ_i and final sparsity θ_f, respectively via ERK.
$\mathbf{W}' = \mathbf{W}'_1, \mathbf{W}'_2, ..., \mathbf{W}'_L \leftarrow$ sparsify $\mathbf{W}_1, \mathbf{W}_2, ..., \mathbf{W}_L$ with P_i
for each training iteration t **do**
  Loss $E \leftarrow g(x_t, \mathbf{W}')$, $x_t \in \mathcal{X}$
  if t (mod ΔT) == 0 and $t < T_{end}$ **then**
    for $1 \leq l \leq L$ **do**
      Calculate the number of weights to drop $D_{t/\Delta T}^l$ using Equation 5 6 7
      $\mathbf{W}'_i \leftarrow$ ArgDrop($\mathbf{W}'_i$,ArgTopK($\mathbf{W}'_i, D_{t/\Delta T}^l$))
      Calculate the number of weights to grow $G_{t/\Delta T}^l$ using Equation 8 9
      Calculate gradient $\mathbf{Grad}_l$ by equation (2c)
      $\mathbf{W}'_l \leftarrow$ArgGrow($\mathbf{W}'_l$,ArgTopK($\mathbf{Grad}_l \cdot (\mathbf{M}_l == 0), G_{t/\Delta T}^l$))
    end for
  else
    $\mathbf{W}'_l \leftarrow \mathbf{W}'_l - \alpha \nabla(\mathbf{W}'_l)\delta_t$
  end if
end for

D. Memory Footprint Analysis

We further investigate the training efficiency of our proposed method in terms of memory footprint. Suppose a sparse SNN model with a sparsity ratio (the percentage of number of zeros in weight) of $\theta \in [0, 1]$. In each round of forward and backward propagation, N weights and tN gradients are saved. For training, we use single precision (FP32) for weights and gradients to guarantee training accuracy. For inference, the weight precision b_w is platform/implementation specific, for example Intel Loihi uses 8 bits [15], mixed-signal design HICANN [27] has 4 bits for weights, FPGA-based designs such as [28] employes mixed precision (4 bits - 16 bits). For sparse models, we use indices (denoted by b_{idx}-bit numbers) to represent the sparse topology of weights/gradients within the dense model. Compressed sparse row (CSR) is a commonly used sparse matrix storage format.

Consider a 2-D weight tensor reshaping from a 4-D tensor. Each row of the 2-D weight tensor denotes the weight from a filter. For the l-th layer, we denote F_l, Ch_l, and K_l as the number of filters (output channels), number of channels (input channels), and kernel size, respectively. Thus, the size of the weight matrix is F_l rows by $Ch_l \cdot K_l^2$ columns. Thus, the total number of indices of the entire network is $(1 - \theta) \cdot N + \sum_l (F_l + 1)$. And the memory footprint of model representation together with gradients for unstructured sparsity is $(1 - \theta) \cdot ((1 + t)N \cdot b_w + N \cdot b_{idx}) + \sum_l ((F_l + 1) \cdot b_{idx})$. Since the number of filters is much smaller than the total number of weights, we approximate the memory footprint as $(1-\theta) \cdot ((1+t)N \cdot b_w + N \cdot b_{idx})$. Given same timestep t, higher sparsity means the lower memory overhead, which support the effectiveness of proposed method in reducing training memory since it has much higher training sparsity than SOTAs.

IV. Experimental Results

A. Experimental Setup

1) Architectures and Datasets.: We evaluate NDSNN on two popular neural network architectures (i.e., VGG-16 and ResNet-19) for three datasets (i.e., CIFAR-10, CIFAR-100 and Tiny-ImageNet). For fair comparison, we set the total number of training epochs as 300 on both CIFAR-10 and CIFAR-100, while as 100 on Tiny-ImageNet as LTH-SNN. We use SGD as the optimizer while setting the momentum as 0.9 and weight decay as $5e-4$. Also, we follow the setting in [7] and set the training batch size as 128, initial learning rate as $3e-1$ and timesteps as 5 across all experiments.

2) Baselines.: We train VGG-16 / ResNet-19 dense SNNs on various datasets and use them as our dense baselines. Other baselines are divided into two types based on the initial sparsity status of the training process (i.e., dense or sparse). For the former, we choose the SOTA pruning methods (i.e., LTH and ADMM) on SNN. For the latter, we implement the sparse training methods (i.e., SET [24], RigL [26]) on SNN models (i.e., SET-SNN, RigL-SNN).

3) Evaluation Platform: We conduct all experiments using PyTorch with CUDA 11.4 on Quadro RTX6000 GPU and

Dataset	CIFAR-10				CIFAR-100				Tiny-ImageNet			
Sparsity ratio	90%	95%	98%	99%	90%	95%	98%	99%	90%	95%	98%	99%
VGG-16(Dense)		92.59				69.86				39.45		
LTH-SNN [11]	89.77	89.97	88.97	88.07	64.41	64.84	62.97	51.31	38.01	37.51	35.66	30.98
SET-SNN [24]	91.22	90.41	87.26	83.40	66.52	63.48	58.04	50.83	38.80	37.34	33.40	26.74
RigL-SNN [26]	91.64	90.06	87.30	84.08	66.59	63.47	58.21	52.26	38.96	37.75	32.94	28.39
NDSNN (Ours)	**91.84**	**91.31**	**89.62**	**88.13**	**68.07**	**66.73**	**63.51**	**58.07**	**39.12**	**37.77**	**36.23**	**33.84**
ResNet-19(Dense)		91.10				71.94				50.32		
LTH-SNN [11]	87.57	87.16	85.91	82.29	54.66	54.78	42.10	41.46	38.40	37.74	31.34	21.44
SET-SNN [24]	90.79	90.07	87.24	83.17	68.12	64.65	57.49	49.11	49.46	42.13	37.25	27.79
RigL-SNN [26]	90.69	90.02	87.19	83.26	67.33	65.23	56.96	47.96	**49.49**	40.40	37.98	24.13
NDSNN (Ours)	**91.13**	**90.47**	**88.61**	**86.30**	**70.08**	**68.95**	**65.48**	**59.61**	49.25	**47.45**	**45.09**	**41.96**

TABLE I: Test accuracy of sparse VGG-16 and ResNet-19 on CIFAR-10, CIFAR-100, Tiny-ImageNet datasets. The highest test accuracy scores are marked in bold. The LTH-SNN results are our reproduced accuracy using method from [7].

Intel(R) Xeon(R) Gold 6244 @ 3.60GHz CPU. We use SpikingJelly [29] package for SNNs implementation.

B. Accuracy Evaluations of NDSNN

1) CIFAR-10 and CIFAR-100: Evaluation results on CIFAR-10 and CIFAR-100 using VGG-16 and ResNet-19 are shown in Table I. We compare NDSNN with baselines at sparsity ratios of 90%, 95%, 98% and 99% on different models and datasets. Experimental results show that NDSNN outperforms the SOTA baselines on each dataset for VGG-16 and ResNet-19. Specifically, on CIFAR-100, for VGG-16, our proposed method has up to 3.66%, 3.26%, 5.47%, 7.24% increase in accuracy (that is relatively 5.68%, 5.14%, 9.42% and 14.24% higher accuracy) at four different sparsity, respectively. While for ResNet-19, NDSNN has 15.42%, 14.17%, 23.88% and 18.15% increase in accuracy (that is relatively 28.2%, 14.17%, 23.38%, 18.15% higher accuracy) compared to LTH-SNN, obtains 1.96%, 4.30%, 7.99%, 10.5% higher accuracy than SET-SNN and achieves 2.75%, 3.72%, 8.52%, 11.65% higher accuracy than RigL-SNN at a sparsity of 90%, 95%, 98% and 99%, respectively. On CIFAR-10, for VGG-16, NDSNN has up to 2.07%, 1.34%, 2.36%, 4.73% relatively higher accuracy than SOTA at sparsity of 90%, 95%, 98% and 99%, respectively. While for ResNet-19, NDSNN has even higher accuracy than the dense model at a sparsity of 90% and achieves the highest accuracy compared to other baselines at different sparsity.

2) Tiny-ImageNet: The accuracy results on Tiny-ImageNet are shown in Table I. Overall, for both VGG-16 and ResNet-19, NDSNN outperforms other baselines. More specifically, for VGG-16, NDSNN has up to 7.1% higher accuracy than other methods at a sparsity of 99%. For ResNet-19, NDSNN has 10.85%, 9.71%, 13.75%, 20.52% higher accuracy than LTH-SNN at sparsity of 90%, 95% and 98%, 99%, respectively. Compared to SET-SNN, NDSNN has 7.10% and 14.17% increase in accuracy at the sparsity of 99% for VGG-16 and ResNet-19, independently. Compared to RigL-SNN, NDSNN has up to 5.45% and 17.83% increase in accuracy at a sparsity of 99% for VGG-16 and ResNet-19, respectively.

3) Comparison with ADMM Pruning: We compare NDSNN with ADMM pruning using data from [6] as shown in Table II. It can be seen that the accuracy loss become noticeable when the sparsity reaches 75% on CIFAR-10 using LeNet-5. However, the accuracy loss is almost 0 on CIFAR-10 using VGG-16 at the sparsity of 75% which indicates that NDSNN has less accuracy loss when achieving the same sparsity.

Dataset	CIFAR-10			
Sparsity ratio	40%	50%	60%	75%
LeNet-5(Dense)		89.53		
ADMM [6]	89.75	89.15	88.35	87.38
Acc. Loss (%)	0.18	-0.38	-1.18	-2.15
VGG-16(Dense)		92.59		
NDSNN (ours)	92.46	92.32	92.33	92.18
Acc. Loss (%)	-0.001	-0.003	-0.003	-0.004

TABLE II: Comparison of ADMM with NDSNN on CIFAR-10.

C. Efficiency Evaluations of NDSNN

We quantitatively analyze the training cost of dense SNN model, LTH and NDSNN, as showed in Fig. 5. Since no computation is required if there is no input spikes or a connection is pruned. Such that the relative computation cost of sparse model with respect to dense model at training epoch i can be calculated as: $[R_s^i \times Sparsity_i]/R_d^i$, where R_s^i or R_d^i is the average spike rate of the sparse model (LTH/NDSNN) or the dense model at epoch i, which can be tracked throughout entire training. $Sparsity_i$ is the sparsity of the model. On CIFAR 10, the training cost of NDSNN VGG-16 is 10.5% of training a dense model. The cost of NDSNN on ResNet-19 and VGG-16 is 40.89% and 31.35% of LTH, respectively. On CIFAR 100, the training cost of NDSNN ResNet-19 is 27.63% and 40.12% of dense model and LTH respectively; The training cost of NDSNN VGG-16 is 11.87% and 36.16% of dense model and LTH respctively.

D. Design Exploration

1) Effects of Different Initial Sparsity: As the initial sparsity has influence on the average training sparsity, thus the overall training cost. we study the effects of different initial sparsity on accuracy and training FLOPs. Experimental results on VGG-16 / ResNet-19 models and CIFAR-10 / CIFAR-100 datasets are shown in Table III. It's observed that the accuracy gap is small for different initial sparsity. For high training sparsity, we choose initial sparsity from {0.6, 0.7, 0.8} for experiments on CIFAR-10 / CIFAR-100 / TinyImageNet.

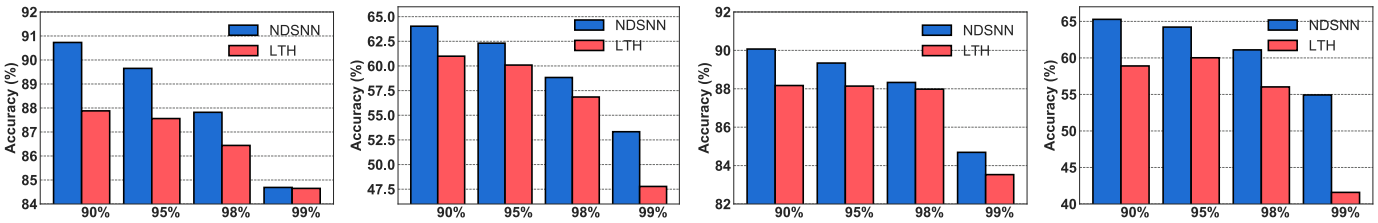

Fig. 4: Comparison of the accuracy of NDSNN and LTH for different sparsity when trained with smaller timestep (timestep=2) on different models and datasets. (a) VGG-16/CIFAR-10. (b) VGG-16/CIFAR-100. (c) ResNet-19/CIFAR-10. (d) ResNet-19/CIFAR-100

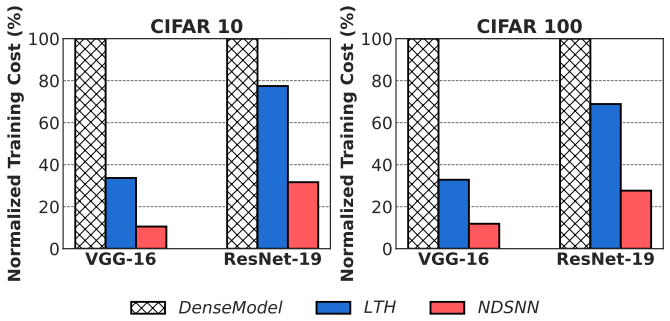

Fig. 5: Training cost comparison on CIFAR-10/CIFAR-100 using VGG-16 and ResNet-19.

Target sparsity	Initial sparsity	VGG-16 CIFAR-10	VGG-16 CIFAR-100	ResNet-19 CIFAR-10	ResNet-19 CIFAR-100
0.95	0.9	90.36	64.52	89.97	66.09
	0.8	91.02	65.74	90.21	67.59
	0.7	**91.31**	66.57	90.47	68.30
	0.6	91.11	66.73	90.56	**68.95**
	0.5	90.94	**66.82**	**90.57**	68.39
0.98	0.9	89.13	61.92	88.58	63.25
	0.8	**89.62**	**63.51**	**88.61**	64.39
	0.7	89.56	63.21	88.48	**65.48**
	0.6	89.50	62.69	88.25	64.74
	0.5	89.48	63.13	88.10	74.89

TABLE III: Study on effects on different initial sparsity.

2) Effects of Smaller Timesteps: We compare the accuracy performance of NDSNN and LTH on a smaller timestep (i.e., $t = 2$) to further validate the effectiveness of proposed method on a more efficient training approach (i.e., the smaller training timesteps, the smaller training cost in time) as shown in Fig. 4. It's observed that NDSNN outperforms LTH on the four experiments (i.e., VGG-16/CIFAR-10, VGG-16/CIFAR-100, ResNet-19/CIAFR-10, ResNet-19/CIAFR-100). On CIFAR-100, NDSNN has 5.55% and 13.34% improvements in accuracy at a sparsity of 99% on VGG-16 and ResNet-19, respectively.

V. Conclusion

In this paper, we propose a novel, computationally efficient, sparse training regime, Neurogenesis Dynamics-inspired Spiking Neural Network training acceleration framework, NDSNN. Our proposed method trains a model from scratch using dynamic sparsity. Within our method, we create a drop-and-grow strategy which is biologically motivated by neurogenesis to promote weight reduction. Our method gives higher accuracy and is computationally less demanding than competing approaches. For example, on CIFAR-100, we can achieve an average increase in accuracy of 13.71% over LTH for ResNet-19 across all sparsities. For all datasets, DNSNN has an average of 6.72% accuracy improvement and 59.9% training cost reduction on ResNet-19. Overall, NDSNN could shed light on energy efficient SNN training on edge devices.

Acknowledgement

This work is partially supported by the National Science Foundation (NSF) under Award CCF-2011236, and Award CCF-2006748.

References

[1] Thomas K Finley. The democratization of artificial intelligence: One library's approach. *ITL*, 2019.
[2] Shanglin Zhou, Bingbing Li, Caiwu Ding, Lu Lu, and Caiwen Ding. An efficient deep reinforcement learning framework for uavs. In *2020 21st International Symposium on Quality Electronic Design (ISQED)*, pages 323–328. IEEE, 2020.
[3] Andreas K Fidjeland and et.al. Accelerated simulation of spiking neural networks using gpus. In *IJCNN*, pages 1–8. IEEE, 2010.
[4] Panjie Qi and et.al. Accelerating framework of transformer by hardware design and model compression co-optimization. In *ICCAD*, pages 1–9. IEEE, 2021.
[5] Panjie Qi and et.al. Accommodating transformer onto fpga: Coupling the balanced model compression and fpga-implementation optimization. In *GLSVLSI*, pages 163–168, 2021.
[6] Lei Deng and et.al. Comprehensive snn compression using admm optimization and activity regularization. *TNNLS*, 2021.
[7] Youngeun Kim and et.al. Exploring lottery ticket hypothesis in spiking neural networks. In *ECCV*, 2022.
[8] Hongwu Peng and et.al. Accelerating transformer-based deep learning models on fpgas using column balanced block pruning. In *ISQED*. IEEE, 2021.
[9] Shiyang Chen and et.al. Et: re-thinking self-attention for transformer models on gpus. In *SC*, pages 1–18, 2021.
[10] Yixuan Luo and et.al. Codg-reram: An algorithm-hardware co-design to accelerate semi-structured gnns on reram. In *ICCD*, pages 280–289. IEEE, 2022.
[11] Jonathan Frankle and et.al. The lottery ticket hypothesis: Finding sparse, trainable neural networks. In *ICLR*, 2018.
[12] Shaoyi Huang and et.al. Sparse progressive distillation: Resolving overfitting under pretrain-and-finetune paradigm. In *ACL*, pages 190–200, 2022.
[13] Guo-li Ming and et.al. Adult neurogenesis in the mammalian brain: significant answers and significant questions. *Neuron*, 2011.
[14] Kirsty L Spalding and et.al. Dynamics of hippocampal neurogenesis in adult humans. *Cell*, 153(6):1219–1227, 2013.
[15] Mike Davies and et.al. Loihi: A neuromorphic manycore processor with on-chip learning. *IEEE Micro*, 2018.
[16] Nitin Rathi and et.al. Stdp-based pruning of connections and weight quantization in spiking neural networks for energy-efficient recognition. *IEEE TCAD*, 2018.
[17] Thao NN Nguyen and et.al. Connection pruning for deep spiking neural networks with on-chip learning. In *ICNS*, 2021.
[18] Emre O Neftci and et.al. Surrogate gradient learning in spiking neural networks: Bringing the power of gradient-based optimization to spiking neural networks. *IEEE SPM*, 2019.
[19] Wei Fang and et.al. Deep residual learning in spiking neural networks. *NeurIPS*, 2021.
[20] Shiwei Liu and et.al. Do we actually need dense over-parameterization? in-time over-parameterization in sparse training. In *ICML*, pages 6989–7000. PMLR, 2021.
[21] Shiwei Liu and et.al. Sparse training via boosting pruning plasticity with neuroregeneration. *NeurIPS*, 34:9908–9922, 2021.
[22] Hongwu Peng and et.al. Towards sparsification of graph neural networks. In *ICCD*, pages 272–279. IEEE, 2022.
[23] Shaoyi Huang and et.al. Dynamic sparse training via balancing the exploration-exploitation trade-off. *arXiv preprint arXiv:2211.16667*, 2022.
[24] Decebal Constantin Mocanu and et.al. Scalable training of artificial neural networks with adaptive sparse connectivity inspired by network science. *Nature communications*, 2018.

[25] Ilya Loshchilov and Frank Hutter. Sgdr: Stochastic gradient descent with warm restarts. In *ICLR*, 2017.
[26] Utku Evci and et.al. Rigging the lottery: Making all tickets winners. In *ICML*, 2020.
[27] Johannes Schemmel and et.al. Wafer-scale integration of analog neural networks. In *IJCNN*, 2008.
[28] Sathish Panchapakesan and et.al. Syncnn: Evaluating and accelerating spiking neural networks on fpgas. *TRETS*, 2022.
[29] Wei Fang and et.al. Spikingjelly. https://github.com/fangwei123456/spikingjelly, 2020.